DOKLADY EARTH SCIENCES, 2025, Vol. 520, No. 1, pp. 151–158

PHYSICS OF THE EARTH

THERMAL CONVECTION MODELING OF THE EVOLUTION OF THE EARTH CORE

© 2025 Academician of RAS L. Ya. Aranovich[a, *] and V. D. Kotelkin[b, **]

Received September 26, 2024
Revised September 27, 2024
Accepted September 30, 2024

Abstract. We present a purely thermal convection 2-D model of the Earth's liquid core, occurring on the background of the secular cooling of the planet. The model includes equations of thermal convection in the Boussinesq approximation and the Coriolis force. Metallic iron with 0.9 wt. % H is chosen for the core composition. The results of modeling show that large vortexes, the 2-D analogues of Taylor columns, are formed in the liquid core prior to crystallization, which might be responsible for the early Earth magnetic field. The early stages of the solid core crystallization are characterized by a chaotic and shapeless growth. Continuing growth of the solid core results in rearrangement of the convection structure decreasing its average velocity but increasing heat flow at the core-mantle boundary due to increased amount of heat of crystallization. The solid core reaches its present size in 0.5 Gy. Averaged temperature profile of the modern liquid core differs significantly from the adiabatic.

Keywords: *thermal convection, liquid core, 2-D modeling, solid core crystallization*

DOI: 10.31857/S26867397250119e8

INTRODUCTION

The onset of crystallization and growth of the solid core is one of the most important events in the endogenous geological history of our planet. It determined the change in the intensity of Earth's magnetic field [1, 2], the magnitude of heat flow at the boundary between the liquid core and mantle (CMB) [6], as well as the nature of interaction between the liquid core and mantle material [4, 6] due to the fractionation of light elements between the solid and liquid core at their boundary (ICB) [5].

Modern estimates of the age (and, consequently, the growth rate) of the solid inner core vary greatly from > 2.5 Gy [2, 11] to 0.5 Gy [3], depending on the estimation method (paleomagnetic data on the intensity of Earth's magnetic field or thermodynamic calculations), boundary conditions (adiabatic T, constant heat flow at the CMB) and values of physical parameters (primarily the thermal conductivity of the core) used in computational models.

Most of the works devoted to processes in the core are related to modeling the generation of the magnetic field [1]. For this purpose, a system of thermal convection equations in the Boussinesq approximation is used, taking into account the Coriolis force due to Earth's rotation, and magnetic induction (for example, [14] and references therein), interacting through the Lorentz force. Modern models in the complete system of equations additionally include the chemical component of convection caused by the fractionation of elements at the CMB and ICB boundaries [6]. Obviously, the processes occurring in the core and at its boundaries are interconnected and interact in a complex nonlinear manner. At the same time, hydrodynamics plays a major role in them. Therefore, for an adequate understanding of the essence of various processes, it is reasonable, as a first approximation, to study convection in its "pure form," limiting ourselves to only the main factors that significantly affect the flow, namely thermal convection and rotation (i.e., without magnetic field and chemical convection). The proposed work is devoted to solving this problem.

[a] *Institute of Geology of Ore Deposits, Petrography, Mineralogy and Geochemistry, Russian Academy of Sciences, Moscow, Russia*
[b] *Lomonosov Moscow State University, Moscow, Russia*
**e-mail: lyaranov@igem.ru*
***e-mail: kotelkin55@mail.ru*

MODEL OF THERMAL CONVECTION WITH CRYSTALLIZATION IN THE BOUSSINESQ APPROXIMATION

Let us choose characteristic scales: L, v_0, T_0, ρ_0, p_0, g_0, v, k, α, Ω^E, C_V, H (Table 1).

Table 1. Physical values used in model calculations

Name of value	Designation	Value
Length — Earth's core radius	L	$3.5 \cdot 10^6$ m
Gravitational acceleration	g_0	10 m/s^2
Density	ρ_0	$12.5 \cdot 10^3$ kg/m^3
Density jump	$\delta\rho$	$0.5 \cdot 10^3$ kg/m^3
Pressure	p_0	360 GPa
Temperature Temperature perturbations	T_0 δT	5000°K 1000°K
Angular velocity of Earth's rotation	Ω^E	0.73 rad/s
Thermal expansion coefficient	α	10^{-5} 1/K
Heat of phase transition	H	$3 \cdot 10^5$ J/kg
Heat capacity at constant volume	C_V	700 J/(kg · K)

Let's write the thermal convection model in dimensionless form, using similarity criteria accepted in hydrodynamics. In the Boussinesq approximation [20], the thermal convection model includes:

Navier-Stokes equations

$$dV/dt = -eFr^{-1}T - Eu\nabla p/r_0 + Re^{-1}DV + \mathbf{Ro^{-1}}\left[\boldsymbol{e}_z \mathrm{x} V\right] + Cfr; \quad (1)$$

heat conduction equation

$$dT/dt = Pe^{-1}\Delta\mathrm{T} - P_0\, div\mathbf{V} + \mathbf{Cr}dQcr/dt \quad (2)$$

and continuity equation

$$V_r dr_0/dr + r_0\, div\mathbf{V} = 0. \quad (3).$$

In these equations $\rho_0(r)$ and $P_0(r)$ are known distributions of density and pressure, the PREM model [8], V_r is the radial velocity component. It is also taken into account that in the Boussinesq approximation, small density perturbations ($\varepsilon << 1$) are linearly expressed through temperature

$$\rho \approx \rho_0(r)(1 - \varepsilon T). \quad (4).$$

The total pressure $P = P_0 + p$, where $P_0 >> p$, consists of hydrostatic P_0 and dynamic p parts. The equations of motion (1) are written in a rotating coordinate system ($\boldsymbol{e}_z$ is the unit vector of the z axis, directed along Earth's rotation axis), they account for gravity, characterized by the Froude number $Fr = v_0^2/g_0L$, $\varepsilon = \alpha\delta T$; pressure forces, characterized by the Euler number $Eu = p_0/\rho_0 v_0^2$; viscous forces, characterized by the Reynolds number $Re = v_0 L/v$; Coriolis forces, characterized by the Rossby number $Ro = v_0 / 2\Omega^E L$, and centrifugal forces, characterized by the coefficient $Cf = [\Omega^E]2L^2/v_0^2$.

The Peclet number is included in the heat conduction equation $Pe = v_0 L/k$ and the coefficient characterizing the heat of phase transition $Cr = H/(C_V T_0)$. Assuming $p_0 = \rho_0 g_0 L$, we get $Fr{\cdot}Eu = 1$ and exclude the Euler number. Note that in our case ρ_0, g_0, L are such that $\boldsymbol{p_0} \approx p_{max} = 360$ GPa equals the pressure at the center of the Earth. The Rayleigh number is expressed through the similarity criteria used $Ra = \varepsilon Fr^{-1} RePe$

It should be noted that with a large linear dimension of the problem, despite the uncertainty of viscosity and thermal conductivity coefficients, the Reynolds Re and Peclet Pe numbers are very large, greater than 10^{10}, so that intense turbulent convection of essentially inviscid and non-heat-conducting fluid occurs in the liquid part of the core. Viscosity and thermal conductivity play a role only in thin boundary layers near solid surfaces. Note that numerical modeling introduces scheme diffusion dependent on the grid step, therefore we will be forced to limit ourselves to Reynolds and Peclet numbers $Re = Pe = 10^6$. The remaining coefficients in our equations are equal to: $Eu = Fr^{-1} = g_0L / v_0^2 = 1.4{\cdot}10^6$, $\varepsilon = 0.01$, $Ro^{-1} = 2\Omega^E L / v_0 = 102$.

INITIAL VALUES AND BOUNDARY CONDITIONS

To complete the problem formulation, it is necessary to set initial values, boundary conditions, and the phase transition condition. The outer radius of the core and the rotation speed of the Earth will be considered constant, i.e., we use simplified model conditions.

Conditions at the boundary with the mantle are the no-slip condition for the velocity vector and the condition for temperature. We will consider the temperature to be the same at all points of the outer boundary and slowly decreasing exponentially with time:

$$T_{\mathrm{CMB}}(t) = T_{\mathrm{CMB}}(0) \cdot \exp(-\lambda_M t). \quad (10)$$

Then the cooling rate will be regulated by the exponent λ_M. It is clear that the mantle, justifying its name, shields the heat output from the core

and slows down the cooling of the planet, so the exponent λ_M must be a small value.

To bypass the problem of initial conditions, we first conduct an auxiliary calculation. We set the initial state of rest with small random temperature perturbations, then due to the instability of such a state, movement arises in the system, which will begin to spin up according to the laws of thermal convection. We will continue the calculation until the stabilization of the average flow, i.e., until the state when the initial conditions are forgotten. The velocity distributions $V(r, 0)$ and temperature $T(r, 0)$ obtained in this way will be taken as the initial state for our modeling.

To model the crystallization of the core, it is necessary to specify the dependence of the melting temperature of the core material on hydrostatic pressure. The density deficit and the longitudinal wave velocities of the core, established by seismology [8], indicate the presence of light elements in its composition. One of the most frequently proposed light elements in the Earth's core is hydrogen [10, 12, 19]. The melting temperature of hydrogen-containing iron strongly depends on the composition FeHx, where x is the number of H atoms per formula unit ($0 < x < 1.2$). At $x = 1$ (composition FeH), the melting curve (T – temperature K, P – pressure, GPa) is described by the equation [10]:

$$T1_{\text{melt}} = T_0((P - P_0)/a + 1)^{1/c}, \qquad (11)$$

where $a = 24.6$, $c = 3.8$, $T_0 = 1473$K and $P_0 = 9.5$ GPa. (11)

The equation of melting curves at variable H content was obtained by interpolation between the curve at x=1 (equation 11) and the melting curve of pure Fe according to [13]:

$$T_{\text{melt}} = T1_{\text{melt}} + (d + e \cdot P)\cdot(1 - x), \qquad (12)$$

where $d = 521.7391$, $e = 4.7826$.

According to the estimate [7], the temperature at the present-day CMB boundary with 95% probability lies in the range of 3470–3880°K. Therefore, for modeling the crystallization process, a melting curve with hydrogen content $x = 0.5$ (0.9 wt. % H) was taken, which falls within the specified range of T_{CMB}, and also agrees well with the estimate of density and P-wave velocity in the core [12]. Note that at this stage of modeling, we did not consider the fractionation of the light element between the solid and liquid core.

ON THE NUMERICAL METHOD AND 2D-MODEL

As a tool for our research, we use a 2D variant of our thermal convection model in a "flat core," the plane of which is orthogonal to Earth's rotation axis. Of course, for realistic modeling, particularly for magnetic field generation, full-scale 3D calculations are necessary. But in this work, to establish the basic properties of thermal convection, a simpler and more understandable 2D model is used, which provides complete visualization, and is also faster and more accurate computationally.

Numerical modeling was carried out using the finite-difference method with second-order approximation of partial differential equations on uniform Cartesian grids. Calculations were performed on grids of $512 \cdot 512$ and $1024 \cdot 1024$ nodes, which is sufficient for direct numerical simulation of turbulent regimes and accounting for large Reynolds and Peclet numbers.

Convection in a fully liquid core. In geophysical literature, it is customary to study and determine the radial distributions of parameters in the Earth in its current state, corresponding to the PREM model. For the core temperature, its adiabatic (or isentropic) distribution is calculated and presented. For example, in the classic monograph by V.N. Zharkov [9], the relation $T_{\text{ad}} = \rho^{\gamma}$ with the Grüneisen parameter $\gamma \approx 1.45$ is used. Since convection in the core is not taken into account in such temperature calculations, the question about its actual distribution remains. The core temperature obtained in our convective 2D model depends on time and coordinates; in polar coordinates, it is a function T (t, r, ϕ). To obtain the temperature distribution in the accepted radial form, it is sufficient to average it over the angular coordinate:

$$T_{av}(t, r) = \langle T(t, r, \phi)\rangle.$$

In Fig. 1, in a natural color scale, deviations of temperature from its average distribution are shown on the left, and the Z-component of vorticity is shown on the right. Shades of red here and further represent positive deviation values, blue color shades represent negative values, and the white color corresponds to near-zero values (when maximum values are exceeded, colors cycle).

It can be seen that thin boundary layers form at the boundary with the mantle: a cold thermal layer and a viscous hydrodynamic layer. The heavy cold layer often detaches and begins to sink in the form of multiple small jets. The thin jets merge and enlarge, and this is repeated in a cascade; ultimately,

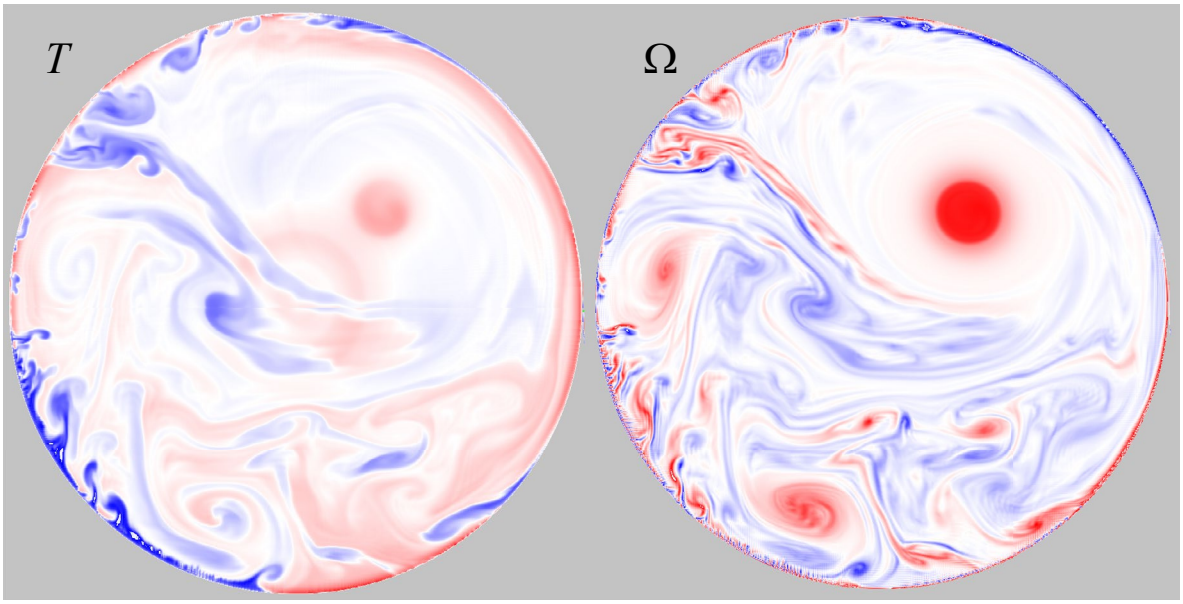

Fig. 1. Temperature (T) and vorticity (Ω) in the core before the onset of crystallization.

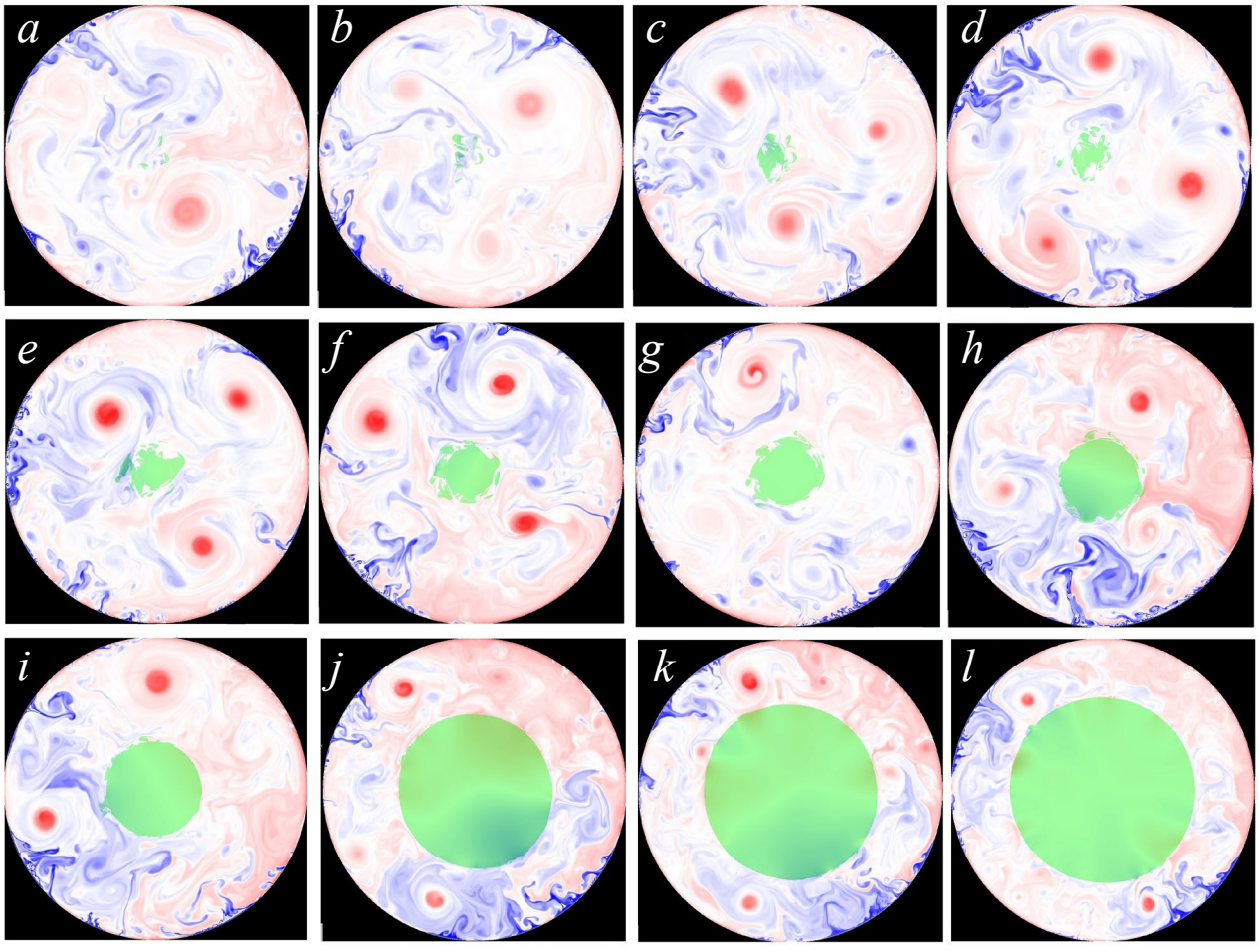

Fig. 2. Sequential stages of core crystallization from early (panel *a*) to late (panel *m*). The modern size of the solid core corresponds to panel *i*.

a small number of rapidly sinking jets remain, which by inertia pass through the weightlessness region in the center and move again toward the mantle, with maximum velocities achieved in the central part (video 1 in the Appendix). Both panels show a characteristic feature of convection in a fully liquid core: the substance does not accumulate in the central part but passes through it by inertia and again exits into the peripheral area.

Small vortices, merging together, enlarge to a size comparable to the core radius. In this regard, it should be noted that there are discrepancies in the literature: some researchers (for example, [4]) note predominantly large-scale organized laminar nature of convection, while others [6, 15] observe small-scale turbulent nature. The results of our modeling show that both regimes occur simultaneously. The large rounded vortices that form in this process are analogues of Taylor vortex columns, which are associated with the generation of a dipole magnetic field [15].

Crystallization modeling. Modeling of the crystallization process on fine grids was carried out as follows. For each node, the melting temperature is known, which depends on the radius through hydrostatic pressure. The grid nodes were divided into "liquid" and "solid" and a Boolean function was introduced to describe their current state. At the beginning of the simulation, all nodes are "liquid." Then, at each moment of time, a check is performed at each node and if the temperature in a liquid node drops below the melting temperature (with a small supercooling), then this node transitions to the category of solid nodes. Similarly, if the temperature in a solid node rises above the melting temperature (with a small overheating), then this node returns to the category of liquid nodes. Each transition is accompanied by the release or absorption of phase transition energy and a jump in density. The increase in the density of the solid phase contributes to its movement and concentration in the central part of the core. In addition, the movement of the solid phase should be rotational-translational and connected to the flow of the liquid phase by adhesion conditions.

Fig. 2 shows the stages of core crystallization in green. It can be seen that crystallization begins in the central region with the appearance of individual crystallization centers, around which crystallizing areas grow, then merging with each other, forming a continuous solidified region.

In more detail, the crystallization process corresponding to our numerical model is shown in video 2 of the Appendix. The crystallizing substance becomes not absolutely solid, but only very viscous. Its density, and with it, gravity also increases slightly. Since there is zero gravity in the central region, the crystallizing substance can, by inertia, cross the crystallization zone, exit it into a low-pressure area, and melt again. However, as the core cools further, the radius of the crystallization zone increases, and solidifying fragments begin to rapidly accumulate in the central region. Liquid layers remain between them, so at this initial stage of crystallization, a loose porous structure is observed in the central region [21]. Later, the liquid layers also crystallize, but this occurs under "zero gravity" conditions. As the solid core grows, the convection structure is restructured; large jets cannot pass through the center and they turn around, partly due to the heat released during crystallization, which increases buoyancy force. Vortex structures twisted by jets decrease in size, resulting in a constant increase in the number of jets and vortex structures. Further growth of the inner core occurs unevenly in places where cold jets approach. Since convection is chaotic, jets approach from different places, and the shape of the crystalline part of the core becomes increasingly round. By the time the inner core reaches its modern size $R = 0.35$ (panel *i* in Fig. 2), its shape becomes almost circular (panels *j, k, l* in Fig. 2; video 2 of the Appendix).

Convection in the core of modern configuration. Convection in the core of modern configuration (the modern radius of the solid core is 1221.5 km, which is 0.35 of the radius of the entire core) is studied most frequently. In particular, there are similar studies in a purely thermal formulation, without considering the magnetic field [17]. The results of modeling thermal convection in the modern core are shown in Fig. 3. Unlike a completely liquid core (Fig. 1), hot ascending flows are added to the cold descending flows. It can be seen that the maximum size of the vortices decreases.

INTEGRAL MODELING RESULTS

2D modeling of the thermal evolution of the core, with the condition of exponentially decreasing temperature at the core/mantle boundary, allows finding complete distributions of temperature, velocities, and phase configurations at all points in time. Videos of numerical experiments are provided in the appendix. For the analysis of results obtained at each point in time, the spatially averaged convection velocity V_{av}, the Nusselt number averaged along the CMB Nu, representing the dimensionless heat flux, and the solid phase area

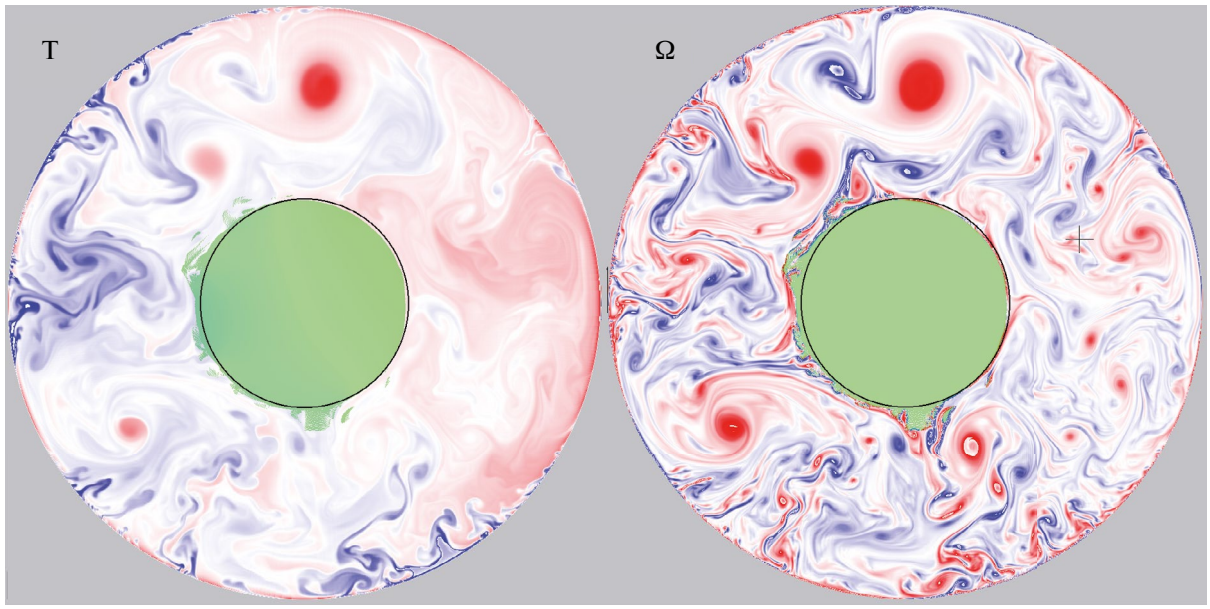

Fig. 3. Temperature (T) and vorticity (W) in the liquid core of the modern configuration.

normalized to the circle radius R_{ic} were additionally calculated (Fig. 4a). The distributions are given in relative variables, with the reference point being the current state t = 0, $R_{ic} = 0.35$.

In our calculations, it is assumed that the CMB temperature decreases exponentially with time (black curve in Fig. 4 on the left). The heat output from the core, i.e., the times of its cooling and crystallization, is controlled by the mantle. To convert the results into dimensional time, additional information about the thermal insulating effect of the mantle, not related to the core, is needed. For example, in [18] it is stated that the gradual cooling of the Earth is about 100° C per billion years. In the work on modeling mantle convection [16], where the first 0.5 billion years are devoted to the crystallization of the mantle itself, it is shown that over the subsequent 4 billion years of geological evolution, the core temperature decreased by 12.5%, which is consistent with the estimate in [18]. This means that 4 billion years ago it was equal to 4434° K. Based on such a cooling rate of T_{CMB}, according to Fig. 4, we find that to reach the current radius of the solid core, its crystallization must have begun approximately 0.5 billion years ago.

The results of the numerical experiment presented in the left part of Fig. 4 show that since the appearance of the solid core, the heat flux from

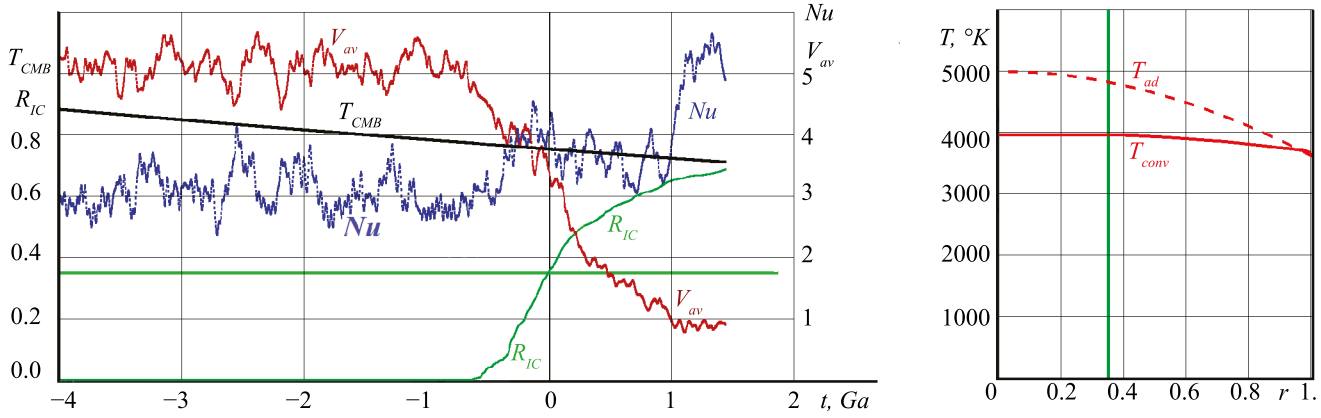

Fig. 4. (left) growth of the inner core (R_{ic}, green color), heat flux from the core to the mantle (Nu, blue) and average convection velocity (V_{av}, brown); (right) – averaged temperature profile in the core (T_{conv}, solid red curve) compared to the adiabatic profile according to [9] (T_{ad}, dashed line).

the core to the mantle increases due to the release of crystallization heat, while the convection velocity begins to decrease, but this happens gradually as the solid core grows, which serves as an obstacle to convection. The chaotically oscillating nature of heat and mass transfer processes is also visible.

The modeling of thermal convection in the liquid core shows that developed turbulent convection occurs at very high velocities, approximately $v_0 \sim 5–7$ m/sec and is accompanied by short-wave oscillations of both the core's moment of inertia and its rotational moment. These oscillations should result in compensating oscillations of the mantle's angular velocity, which are registered on the planet's surface [22].

The distribution of the angular-averaged temperature in the modern liquid core is shown in Fig. 4 on the right. It is evident that as a result of intensive convection, the temperature distribution is flatter compared to the adiabatic one, which is most often used in literature [9]! And this temperature decreases over time.

CONCLUSIONS

The conducted modeling of purely thermal convection has revealed some important features of the evolution of processes that occurred in the Earth's core against the background of planetary cooling.

1. In the liquid outer core, even before the crystallization of the inner core begins, large vortices form, which are two-dimensional analogues of Taylor vortex columns, with which the generation of a dipole magnetic field is associated. That is, the emergence of Earth's magnetic field may not be directly related to the formation of the solid core. This result may resolve contradictions between estimates of the age of existence of Earth's magnetic field.

2. Rapid chaotic growth of the solid core at the initial stage of crystallization.

3. The amorphous configuration of the core at the initial stage of crystallization and its loose structure are naturally explained by the absence of gravity at the center.

4. With the appearance of a solid core that blocks convective flows through the center, the restructuring of the convection pattern begins, and the average convection velocity decreases. However, the heat flux from the core to the mantle increases due to the release of crystallization heat.

5. The averaged temperature profile in the liquid core differs from the adiabatic one.

The model proposed in our work does not include a number of important processes that can significantly affect heat and mass transfer and, consequently, the nature of convection in the core. This is, first of all, the fractionation of the light element (hydrogen) between the solid and liquid core, which generates an important chemical component of convective flows. Secondly, our modeling does not take into account electromagnetic Lorentz forces. In addition, like all previous works known to us, it was conducted under the assumption that the total size of the core corresponds to the modern one, i.e., it did not change over time, and does not take into account the possibility of chemical exchange of metal and light element at the outer core-mantle boundary. Solving these problems is a task for future research.

FUNDING

The research was carried out within the framework of the state assignment of IGEM RAS.

REFERENCES

1. *Aubert J.* State and evolution of the geodynamo from numerical models reaching the physical conditions of Earth's core // Geophysical Journal International. 2023. V. 235. Pp. 468–487. https://doi.org/10.1093/gji/ggad229

2. *Biggin, A., Piispa, E., Pesonen, L., et al.* Palaeomagnetic field intensity variations suggest Mesoproterozoic inner-core nucleation // Nature. 2015. V. 526. Pp. 245–248. https://doi.org/10.1038/nature15523

3. *Bono R.K., Tarduno J.A., Nimmo F., Cottrell R.D.* Young inner core inferred from Ediacaran ultra-low geomagnetic field intensity // Nature Geoscience. 2019. V. 12. Pp. 143–147. doi:10.1038/s41561-018-0288-0

4. *Bouffard M., Choblet G., Labrosse S., Wicht J.* Chemical Convection and Stratification in the Earth's Outer Core // Frontiers in Earth Science. 2019. V. 7:99. doi: 10.3389/feart.2019.00099

5. *Braginsky S.* Structure of the F layer and reasons for convection in the Earth's core // Soviet Physics Doklady. 1963. V. 149. Pp. 8–10.

6. *Davies C.J., Greenwood S.* Dynamics in Earth's Core Arising from Thermo-Chemical Interactions with the Mantle. In: Core - Mantle Co - Evolution: An Interdisciplinary Approach (T.Nakagawa, T.Tsuchiya, M.Satish-Kumar, G.Helffrich Eds). 2023. https://doi.org/10.1002/9781119526919.ch12

7. *Deschamps F., Cobden L.* Estimating core-mantle boundary temperature from seismic shear velocity and attenuation // Frontiers in Earth Science. 2022. V. 10:1031507. doi: 10.3389/feart.2022.1031507

8. *Dziewonski A.M., Anderson D.L.* Preliminary reference Earth model // Physics of the Earth and Planetary Interior. 1981. V. 25. Pp. 297–356. https://doi.org/10.17611/DP/9991844

9. *Zharkov V.N.* Physics of the Earth's interior. Moscow: Science and Education. 2012. 383 p.

10. *Hirose K., Tagawa S., Kuwayama Y. et al.* Hydrogen limits carbon in liquid iron // Geophysical Research Letters. 2019. V. 46. Pp. 5190–5197. https://doi.org/10.1029/2019GL082591

11. *Konôpková Z., McWilliams R.S., Gómez-Pérez N., Goncharov A.F.* Direct measurement of thermal conductivity in solid iron at planetary core conditions // Nature. 2016. V. 534. Pp. 99–101. doi:10.1038/nature18009

12. *Sakamaki K., Takahashi E., Nakajima Y. et al.* Melting phase relation of FeH *x* up to 20 GPa: Implication for the temperature of the Earth's core // Physics of the Earth and Planetary Interior. 2009. V. 174. Pp. 192–201. https://doi.org/10.1016/j.pepi.2008.05.017

13. *Zhang D., Jackson J.M., Zhao J. et al.* Temperature of Earth's core constrained from melting of Fe and Fe0.9Ni0.1 at high pressures // Earth and Planetary Science Letters. 2016. V. 447. Pp. 72–83. https://doi.org/10.1016/j.epsl.2016.04.026

14. *Reshetnyak M.Yu.* Parametric thermal model of Earth's evolution // Astronomy Letters. 2021. V. 47. Pp. 525–534. doi: 10.31857/S032001082107007X

15. *Kirdyashkin A.G., Dobretsov N.L., Kirdyashkin A.A.* Turbulent convection and magnetic field of the Earth's outer core. // Geology and Geophysics. 2000. V. 41. Pp. 601–612.

16. *Kotelkin V.D., Lobkovsky L.I.* Myasnikov's General Theory of Planetary Evolution and Modern Thermochemical Model of Earth's Evolution // Physics of the Earth. 2007. Pp. 26 – 44.

17. *Gorelikov A.V., Ryakhovskiy A.V., Fokin A.S.* Numerical Study of Some Non-Stationary Regimes of Natural Convection in a Rotating Spherical Layer // Computational Continuum Mechanics. 2012. V. 5. Pp. 184–192. doi: 10.7242/1999-6691/2012.5.2.22

18. *Jacobs J.A.* The Earth's inner core // Nature. 1953. V. 172. Pp. 297–298. doi:10.1038/172297a0

19. *Aranovich L.Y., Persikov E.S., Bukhtiyarov P.G., Bondarenko G.S.* Interaction of Fe_3C with Hydrogen: On the Compatibility of Carbon with Hydrogen in Metallic Iron // Petrology. 2021. V. 29. Pp. 695–701. DOI: 10.1134/S0869591121060072

20. *Gershuni G.Z., Zhukhovitskiy E.M.* Convective Stability of Incompressible Fluid. Moscow: Nauka. 1972. 392 p.

21. *Pang G., Koper K.D., Wu S.-M. et al.* Enhanced inner core fine-scale heterogeneity towards Earth's centre // Nature. 2023. V. 620. Pp. 570–575. https://doi.org/10.1038/s41586-023-06213-2

22. *Zotov L., Bizouard Ch., Sidorenkov N. et al.* Multidecadal and 6-year variations of LOD. // Journal of Physics: Conference Series (JPCS). 2020. 1705 012002. IOP Proceedings of FAPM 2019 conference.